Available online at www.sciencedirect.com

SCIENCE @ DIRECT®

Journal of Nuclear Materials 351 (2006) 155–161

journal of nuclear materials

www.elsevier.com/locate/jnucmat

Effect of hafnium on radiation-induced inter-granular segregation in ferritic steel

Z. Lu [a,*], R.G. Faulkner [a], N. Sakaguchi [b], H. Kinoshita [b], H. Takahashi [b], P.E.J. Flewitt [c]

[a] Institute of Polymer Technology and Materials Engineering, Loughborough University, Loughborough, Lecestershire LE11 3TU, UK
[b] Center for Advanced Research of Energy Technology, Hokkaido University, North 13, West 8, Sapporo 060-8628, Japan
[c] Berkeley Centre, Magnox Electric, Berkeley, Gloucestershire GL13 9PB, UK

Abstract

Ferritic steels with and without hafnium (Hf) addition were irradiated by 250 keV nickel ions at 300 °C in an ion accelerator attached to the multi-beam high voltage electron microscope (JEOL ARM1300) to study the influence of Hf additions on radiation-induced segregation in a ferritic/martenitic steel. Grain boundary segregation of phosphorus, silicon, chromium and molybdenum were measured by field-emission-gun transmission electron microscopy with an energy dispersive analyser. The results show that radiation induces the enrichment of undersized atoms (P) and the depletion of oversized atoms (Cr) in the materials without Hf addition. The addition of Hf suppresses radiation-induced undersized atom enrichment and oversized atom depletion. A radiation-induced non-equilibrium segregation (RIS) model is developed to predict undersized and oversized atom segregation behaviour at the grain boundary. The effect of hafnium on freely migrating defect population is discussed and estimated to indicate the effect of the element on segregation behaviour of the elements like P and Cr in the ferritic steel. The predicted results are compared with experimental data.

1. Introduction

Radiation by high energy particles (electrons, ions, neutrons) may induce the redistribution of impurities and solutes near sinks, such as point defects, dislocations and boundaries. The enrichment and/or depletion of the elements at grain boundaries will influence the mechanical properties of materials. The enrichment of undersized impurity atoms, e.g. phosphorus in ferritic reactor pressure vessel steels, reduces the grain boundary cohesion, causing the materials to fail through inter-granular embrittlement [1]. The depletion of oversized solute atoms, e.g. chromium in austenitic steels, is believed to contribute to the irradiation-assisted stress corrosion cracking (IASCC) [2]. It has been found that radiation-induced Cr depletion in austenitic steels and radiation-induced P enrichment in ferritic steels can be suppressed by oversized atom additions [3–10]. Ti, V, Nb, Ta, Zr, Hf and Pt were added to austenitic steels [3–9] and Hf to ferritic steel [10] to study the influence of oversized solute additions on radiation-induced segregation (RIS). Hf and Zr additions show the best suppression effect for Cr

---

[*] Corresponding author. Tel.: +44 1509 223618; fax: +44 1509 223949.
E-mail address: zheng.lu@lboro.ac.uk (Z. Lu).

0022-3115/$ - see front matter © 2006 Elsevier B.V. All rights reserved.
doi:10.1016/j.jnucmat.2006.02.026

depletion in austenitic steels. The majority of work has been focused on austenitic steels so far and few studies of ferritic steels have been made. In this study, the effect of Hf additions on radiation-induced segregation in ferritic steels is investigated. Radiation-induced segregation models (RIS) are also presented to predict the inter-granular segregation of undersized and oversized solute atoms.

2. Experimental

E911 was supplied by Corus in the as-received condition, i.e. normalised at 1060 °C for 1 h, then air cooled. The chemical compositions are listed in Table 1.

Samples used in this study are 3 mm dia. TEM-discs. Electro-polishing was applied to produce thin areas at the edge of holes. Hafnium (Hf) (1 at.%) is implanted in E911 at room temperature. E911 with and without Hf (marked by E911 + Hf and E911, respectively) were irradiated by heavy ion (Ni^+) in the ion beam line attached to the multi-beam high voltage electron microscope (JEOL ARM 1300), Hokkaido University, Japan. Irradiations were carried out at a dose rate of 6.25×10^{12} Ni^+ cm^{-2} s^{-1} at 300 °C. Doses were 8.06×10^{16} Ni^+ cm^{-2}.

A conversion from dose (ion fluence, ions cm^{-2}) to displacement dose (dpa) is given by [11]

$$\mathrm{dpa} = \frac{0.8}{2E_\mathrm{d}}\left(\frac{\mathrm{d}E}{\mathrm{d}x}\right)\frac{\Phi}{\rho},$$

where E_d is a displacement threshold energy (about 40 eV for steel), $\frac{\mathrm{d}E}{\mathrm{d}x}$ is the linear energy transferred per ion to the target by nuclear processes, Φ is ion fluence, ρ is target (steel) atomic density. $\frac{\mathrm{d}E}{\mathrm{d}x}$ is calculated by SRIM 2003. The corresponding dose rate and dose in units of dpa are 2.36×10^{-5} dpa/s and 0.305 dpa.

After irradiation, ion thinning of TEM foils was carried out by an ion-milling instrument in order to remove surface amorphous layers induced by ion implantation. The grain boundary composition was measured using a field-emission-gun analytical TEM (JEOL 2010F) equipped with an energy dispersive X-ray analyzer (Noran Inc. VOYAGER system). The nominal spot size is 0.5 nm.

Table 1
Chemical compositions of E911 steel (wt%)

Cr	C	W	N	Mn	Si	P	S
9.16	0.105	1.00	0.072	0.35	0.2	0.007	0.003
Ni	**Nb**	**Mo**	**V**	**Sn**	**As**	**Sb**	**Fe**
0.23	0.68	1.01	0.23	–	–	–	Bal.

3. Modelling segregation

3.1. RIS for undersized atoms

The binding energy between the self-interstitial and the solute atoms is related to the magnitude and sign of the misfit of the solutes in the complex. The magnitude of RIS is dependent upon the magnitude of binding energy, whilst the distribution is governed by the sign of binding energy. For undersized atoms, the self-interstitial, rather than the vacancy, is regarded as the main transporter of impurities because the migration energies are lower and binding energies are higher than for the vacancy–impurity situation [17,15]. Although recent researches [19,20] show the vacancy–P atom complex also plays a role in RIS, the self-interstitial–impurity mechanism is thought to be dominant in RIS. For undersized solutes, the binding energy is positive and the solutes migrate in the same direction as the self-interstitial. On the basis of the earlier models [10,12], the misorientation and stress effects are included. The maximum segregation, C^j_m, of undersized atoms induced by irradiation at grain boundary in ternary alloys can be expressed by

$$C^j_\mathrm{m} = C^j_\mathrm{g}\frac{E^\mathrm{ip}_{\mathrm{b}(j)}}{E^\mathrm{p}_\mathrm{f}}\left[\frac{C^j_\mathrm{g}\exp\left(\frac{E^\mathrm{ip}_{\mathrm{b}(j)}}{kT}\right)}{\sum_j C^j_\mathrm{g}\exp\left(\frac{E^\mathrm{ip}_{\mathrm{b}(j)}}{kT}\right)}\right] \times\left[1+\frac{\alpha L(t_\mathrm{f})\mathrm{BGF}(\eta)}{A_\mathrm{p}D_\mathrm{p}k^2_\mathrm{dp}}\exp\left(\frac{E^\mathrm{p}_\mathrm{f}}{kT}\right)\right] \quad (j=1,2), \tag{1}$$

where C^j_g is the solute concentration in the matrix; $E^\mathrm{ip}_{\mathrm{b}(j)}$ is the self-interstitial–impurity binding energy; E^p_f is the point-defect formation energy; k is Boltzmann's constant; T is the absolute temperature; α is a misorientation factor, which can be expressed by $\alpha = 1 - \exp(-lE_\mathrm{GB}/kT)$, l is a constant, E_GB is the grain boundary energy; G is the dose rate; B is the dose rate correction factor related to the FMD concentration; $F(\eta)$ is the long-range recombination factor of the freely migrating defect; $L(t_\mathrm{f})$ is the foil effect factor [10]; A_p is a constant associated with the vibrational entropy of atoms around the point-defect; D_p is the diffusion coefficient of point-defects in the matrix; k^2_dp is the sink strength for point-defects; E_f^p is the formation energy of point-defects. The final grain boundary concentration, $C^j(t)^*$, after irradiation time t, including site competition effects between the solutes i and j, is given by [10,12,18]

$$C^j(t)^* = C^j(t)\left(\frac{C_g^j \exp(Q_j/kT)}{C_g^i \exp(Q_i/kT) + C_g^j \exp(Q_j/kT)}\right). \tag{2}$$

Here, $C^j(t)$ is grain boundary concentration after irradiation time, t, without site competition; Q_i and Q_j is the binding energy of grain boundary with the solutes. When a stress is applied at grain boundary, it is assumed the direction of stress is perpendicular to GB, and the binding energy of grain boundary with solutes is expressed by $Q^\sigma = Q - p\Delta V$, here Q is the binding energy without stress, p is the applied tensile (+)/compressive (−) stress, ΔV is the volume of impurity. Effects of free carbon, dose rate, misorientation and stresses on RIS of phosphorus in α-Fe are shown in Fig. 1. Radiation induces a P segregation peak in the temperature range 200–300 °C. At the lower temperature, for example, less than 200 °C, although irradiation produces greater damage, the diffusion coefficient of impurity is low. So RIS is low. At higher temperature, for example, 400 °C, the diffusion coefficient increases but irradiation damage decreases because of defect annihilation. It should be noted that the diffusion mentioned here is enhanced by irradiation. The position of the peak is related to the irradiation condition and materials. The second peak is caused by equilibrium segregation. Fig. 1(a) shows that with the increase of free carbon concentration, radiation-induced P GB segregation decreases. This is because there is site competition between P and C, i.e. C can occupy preferentially the sites on the grain boundary. With the decrease of dose rate, radiation-induced P segregation peak moves towards the lower temperature region (Fig. 1(b)). Different Σ values correspond to different grain boundary energy. α in Eq. (1) is the function of grain boundary energy. So RIS of P at GB with different Σ can be calculated from Eq. (1). In the low Σ boundary, for example, $\Sigma3$, P segregation is low (Fig. 1(c)). The tensile stress enhances GB P segregation, while the compressive stress suppresses GB P segregation (Fig. 1(d)). The P segregation ratio used in Fig. 1 is the ratio of radiation-induced P GB segregation and P bulk concentration.

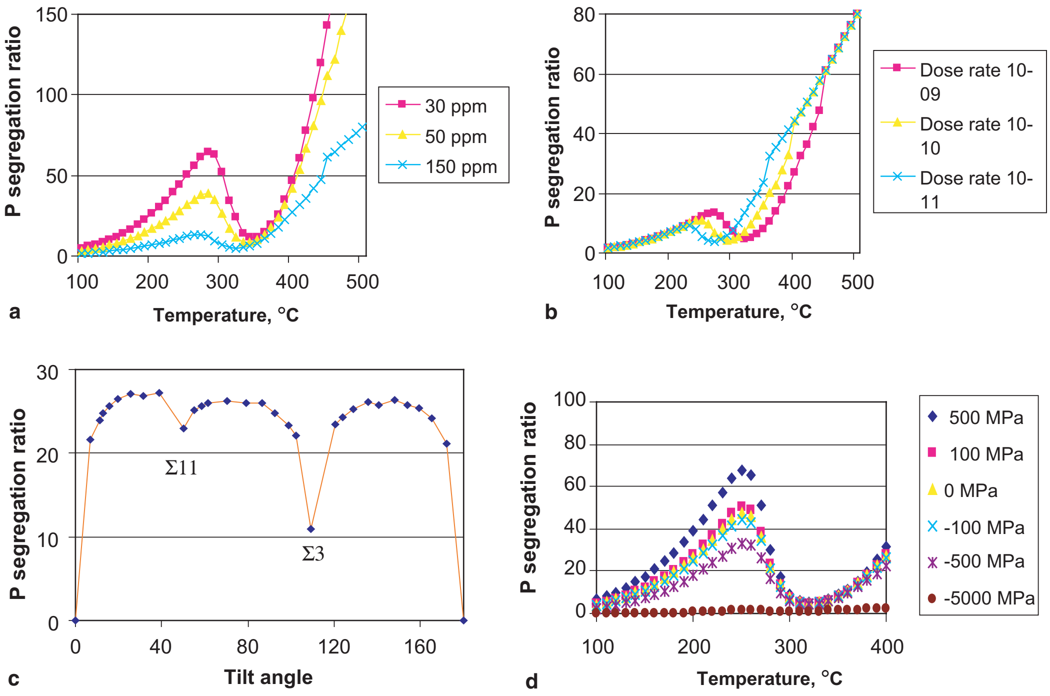

Fig. 1. Effects of free carbon (a), dose rate (b), misorientation (c) and stresses (d) on RIS of P at GB.

3.2. RID of oversized atoms

For oversized atoms, Goodwin and Faulkner's model is used [13,14]. Both interstitials and vacancies are produced during radiation, but only the contribution from interstitial–solute complexes is considered in the model. The detailed discussion on this issue can be found elsewhere [14]. For oversized solutes, the binding energy is negative (Fig. 5) and it is assumed that the solute is repelled by the interstitial and the solutes migrate in the opposite direction to the interstitial. The maximum RIS of oversized atoms at the grain boundary in the binary alloys (site competition is not considered here), C_m, is then given by

$$\frac{1}{C_m}=\frac{1}{C_g}\left[1+\frac{L(t_f)\mathrm{BGF}(\eta)}{AD_pk_{dp}^2}\exp\left(\frac{E_f^p}{kT}\right)\right]. \tag{3}$$

The evaluation of the time dependency of RIS is given by

$$C=C_g+(C_m-C_g)\left[1-\exp\left(\frac{4D_ct}{\alpha^2d^2}\right)\mathrm{erfc}\left(\frac{2\sqrt{D_ct}}{\alpha d}\right)\right], \tag{4}$$

where D_c is the diffusion coefficient of the complex, t is the radiation time, α is the ratio of C_m/C_g and d is grain boundary thickness.

The concentration profile of RIS is given by [13]

$$C_x=C_g\left(\beta+(1-\beta)\mathrm{erf}\left(\frac{x}{2\sqrt{D_ct}}\right)\right), \tag{5}$$

where β is the ratio of C_g/C, and x is the distance from grain boundary.

3.3. Effect of oversized atoms on FMD and consequent segregation behaviour of other elements

Radiation produces an excess of point-defects (vacancies and self-interstitials) in the matrix, while the concentration of point defects at the grain boundary approaches the thermal equilibrium concentration. The point-defects surviving from cascades are called freely migrating point-defects (FMD), which form complexes with solutes and migrate towards GBs. For undersized solute atoms, like P, the binding energy with self-interstitials is higher than that with vacancies. Thus, P-self-interstitial complexes are formed and migrate towards GB. This is radiation-induced segregation (RIS). Oversized solute atoms, like Cr, can form the complexes with self-interstitials and the binding energy is negative. The self-interstitial–solute pairs migrate away from the GB. This is radiation-induced depletion (RID). The binding energies of FMD to various solutes are calculated by using Faulkner's model [15] and are shown in Fig. 5. It is well known that RIS or RID is dependent on FMD concentration through the B in Eq. (1). The oversized addition atoms have positive binding energy with vacancies. With the increase of the radius of addition atoms, the binding energy increases. This means the atoms with larger atomic radius (Hf, Zr) can capture vacancies more easily than the others (Ti, Ta, Nb, V). The capture of vacancies by addition atoms results in reduced mobility of vacancies and enhancement of vacancy–interstitial recombination in the matrix. So the population of FMD decreases and RIS or RID also decreases. This is agreement with experimental observation. The effect of oversized atom addition on the population of FMD can be estimated by

$$\frac{C_{Fe}E_{Fe}^b}{C_{Hf}E_{Hf}^b}=\frac{B_{Hf}}{B},$$

where C_{Fe}, C_{Hf} are the concentration of Fe and Hf in matrix; E_{Fe}^b, E_{Hf}^b are the binding energies of Fe and Hf with vacancies respectively; B is the freely migrating defect concentration in alpha Fe; B_{Hf} is the FMD concentration in the materials with the Hf addition. The calculated B_{Hf} is 0.246B, which means that the population of FMD decreases to about one-quarter of the value for the case without Hf addition. It should be emphasized in addition to FMD being affected by the presence of large atoms, the recombination item $F(\eta)$ and complex diffusion coefficient in Eq. (1) will also be changed. We have not yet included this into the modeling.

4. Results and discussion

Ferritic E911 steel shows a lath martensite microstructure (see Fig. 2). There are a few Nb-rich carbides in E911 (from tens to hundreds of nm in diameter) prior to the irradiation at 300 °C.

The grain boundary composition of unradiated E911, radiated E911 and radiated E911 + Hf was measured. The effect of hafnium on segregation behaviour of undersized and oversized elements is described below.

P is an undersized element in ferritic steels. The P concentration in the matrix is 0.007 wt%. Heat treatment induces P enrichment at the GB

Fig. 2. The microstructure of E911.

(0.17 wt%) measured experimentally. For the materials without Hf addition, radiation at 300 °C results in P segregation towards the GB (up to 1.66 wt%). In the materials with Hf addition, the concentrations of P at the GB are suppressed (0.3 wt%), see Fig. 3.

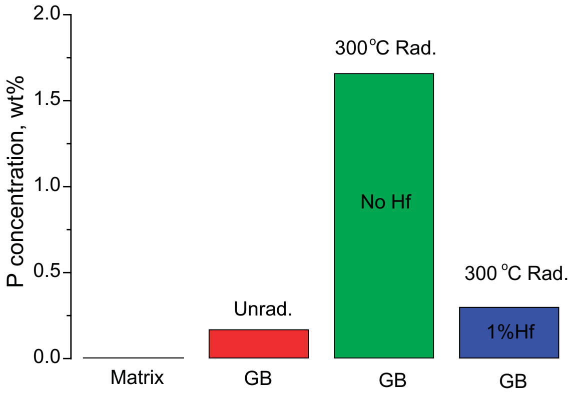

Fig. 3. Phosphorus concentration in unradiated, radiated E911 and radiated E911 + Hf steels.

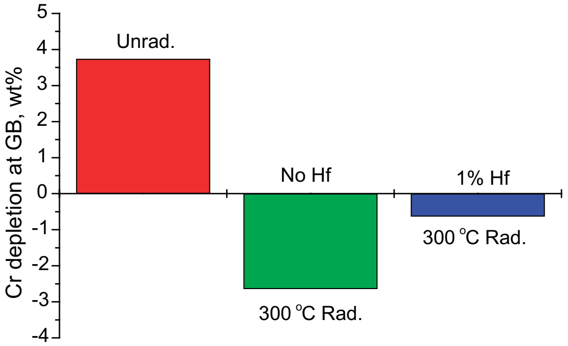

Fig. 4. Cr GB concentrations in unradiated, radiated E911 and radiated E911 + Hf steels.

Table 2
The input data used in the models

Parameter	P	C	Cr
Entropy constant associated with self-interstitial	1	1	1
Vacancy formation energy (eV)	1.4	1.4	1.4
Self-interstitial formation energy (eV)	3.0	3.0	3.0
Self-interstitial–impurity binding energy (eV)	0.57	1.12	–
Impurity diffusion activation energy (eV)	2.68	0.83	2.38
Self-interstitial–impurity complex diffusion activation energy (eV)	0.87	1.42	–
Self-interstitial migration energy (eV)	0.3	0.3	0.3
Pre-exponential diffusion constant for impurities ($m^2 s^{-1}$)	7.12×10^{-3}	3.94×10^{-7}	1.48×10^{-4}
Pre-exponential diffusion constant for complexes ($m^2 s^{-1}$)	8×10^{-7}	8×10^{-7}	8×10^{-7}
Pre-exponential diffusion constant for self-interstitials ($m^2 s^{-1}$)	5×10^{-6}	5×10^{-6}	5×10^{-6}
Self-interstitial bias	1.1	1.1	1.1
Activation energy for dislocation recovery (eV)	0.1	0.1	0.1
Equilibrium segregation parameter	0.775	0.775	–
Binding energy with grain boundary (eV)	0.54	0.829	–
Grain boundary width (nm)	1	1	1

Cr is oversized atom in ferritic steels. The concentration of Cr in the matrix is 9.16 wt%. Prior to radiation, there is enrichment due to heat treatment of Cr (+3.74 wt%) measured experimentally at the GB, similar to the case for P. For the materials without Hf addition, the radiation induces the depletion of Cr (−2.04 wt%) at the GB. In the materials with Hf addition, the depletion of Cr is suppressed (−0.63 wt%) (see Fig. 4).

The radiation-induced undersized P atom and oversized Cr atom inter-granular segregation behaviour is calculated by the models in Section 3. The presence of Hf is accommodated by a revised value of *B*, the FMD concentration, in Eqs. (1) and (3) as indicated in Section 3.3. Input data for modeling can be found in Table 2. The results are shown in Figs. 6 and 7, respectively. Here, the experimental data are corrected according to an analytical convolution method established by Faulkner et al. [16] because the actual segregated solute grain boundary concentration should be much higher or lower in the case of enrichment or depletion than those determined by the FEGTEM microanalysis because of its limited spatial resolution. The calculated results show a good agreement with experimental data when the change of FMD population *B* in the presence of Hf is considered.

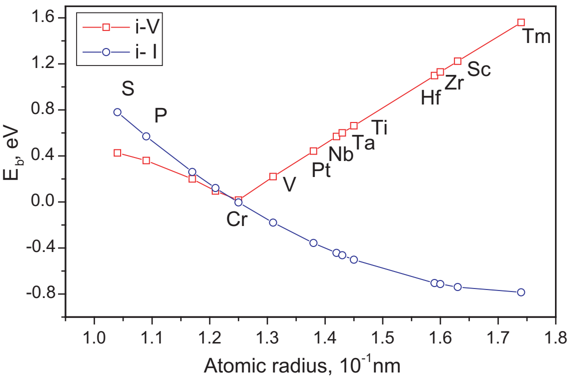

Fig. 5. The binding energies of impurities and point-defects in ferritic steel.

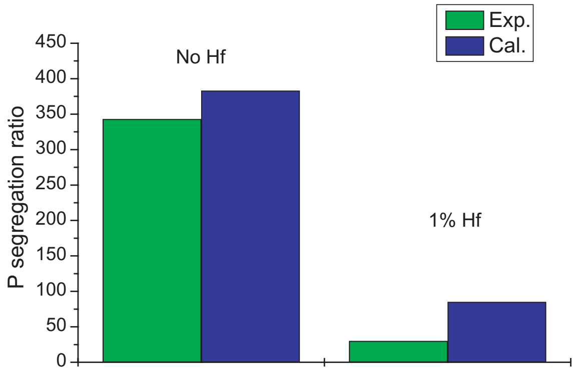

Fig. 6. The comparison of experimental data and predicted results of P enrichment at GB.

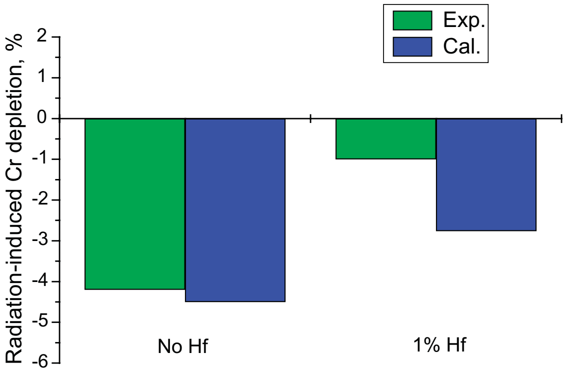

Fig. 7. The comparison of experimental data and predicted results of Cr depletion at GB.

5. Summary

Radiation induces undersized atom (P) enrichment and oversized atom (Cr) depletion at grain boundaries in E911 steel. This phenomenon can be suppressed by the addition of an oversized atom, Hf. The effect of Hf on the population of freely migrating point-defects is estimated. The models for predicting RIS are presented. The predicted results show a good agreement with experimental data.

Acknowledgements

This study is sponsored by EPSRC (contracts GR/R37999 and GR/R01682) and JSPS, Japan.

References

[1] C.A. English, S.R. Ortner, G. Gage, W.L. Server, S.T. Rosinski, ASTM-STP 1405 (2001) 151.
[2] T. Shoji, S. Suzuki, K.S. Raja, J. Nucl. Mater. 258–263 (1998) 241.
[3] T. Kato, H. Takahashi, M. Izumiya, Mater. Trans. JIM 32 (1991) 921.
[4] T. Kato, H. Takahashi, M. Izumiya, J. Nucl. Mater. 189 (1992) 167.
[5] T. Kato, H. Takahashi, M. Izumiya, J. At. Energy Soc. Jpn. 34 (1992) 889.

[6] L. Fournier, B.H. Sencer, G.S. Was, E.P. Simonen, S.M. Bruemmer, J. Nucl. Mater. 321 (2003) 192.

[7] N. Shigenaka, S. Ono, Y. Isobe, T. Hashimoto, H. Fujimori, S. Uchida, J. Nucl. Sci. Technol. 33 (1996) 577.

[8] H. Watanabe, T. Muroga, N. Yoshida, J. Nucl. Mater. 239 (1996) 95.

[9] S. Dumbill, W. HanksProceedings of the Sixth International Symposium on Environmental Degradation of Materials in Nuclear Power System – Water Reactors, The Minerals, Metal and Materials Society, San Diego, CA, 1993, p. 521. August 1–5.

[10] Z. Lu, R.G. Faulkner, N. Sakaguchi, H. Kinoshita, H. Takahashi, P.E.J. Flewitt, J. Nucl. Mater. 329–333 (2004) 1017.

[11] E.H. Lee, Nucl. Instrum. and Meth. B 151 (1999) 29.

[12] R.G. Faulkner, S. Song, P.E.J. Flewitt, M. Victoria, P. Marmy, J. Nucl. Mater. 255 (1998) 189.

[13] C.C. Goodwin, Ph. D. Thesis, 1998.

[14] C.C. Goodwin, R.G. Faulkner, S.B. Fisher, ASTM-STP 1325 (1999) 634.

[15] R.G. Faulkner, S.H. Song, P.E.J. Flewitt, Mater. Sci. Techol. 12 (1996) 904.

[16] R.G. Faulkner, T.S. Morgan, E.A. Little, X-ray Spectrom. 23 (1994) 195.

[17] R.G. Faulkner, P.E.J. Flewitt, Z. Lu, ASTM-STP 1447 (2004) 553.

[18] R.G. Faulkner, R.B. Jones, Z. Lu, P.E.J. Flewitt, Philos. Mag. 85 (2005) 2065.

[19] G.J. Ackland, M.I. Mendelev, D.J. Srolovitz, S. Han, A.V. Barashev, J. Phys.: Condens. Matter. 16 (2004) S2629.

[20] A.V. Barashev, in: Conference Proceedings of Second International Conference on Multiscale Materials Modeling, 11–15 October, 2004, p. 483.